

composition, phase identification, and infrared spectrum of absorption or emission of sodium bentonite. It is essential to identify the behavior and adsorption capacity of clay samples in catalyzed reactions for better utilization. Change in infrared spectrum provides information on the mechanism as the difference of the spectra of nano-particles adsorbed on the surface of the clay. The physico-chemical properties are also calculated for further understanding of samples useful for the thermo-catalytic waste valorization of plastic wastes. The cost of the sodium bentonite clay is comparatively lower as compared to the kaolin. A comparative analysis is done throughout the impurities present in the samples for an effective influence of clays used as the catalyst in thermo-catalytic pyrolysis of waste plastics valorization.

II. 2. EXPERIMENTAL WORKS

2.1 Materials

Sodium bentonite belongs to the smectite group of clay has a similar structure of pyrophyllite. The clay used in this study was procured from Heilen Biopharm Pvt. Ltd, Gujrat, India. The composition of the sodium bentonite sample is as follows: 52.55% SiO₂, 15.34% Al₂O₃, 0.29% K₂O, 11.92% Fe₂O₃, 1.6% TiO₂, 2.75 % MgO, 1.4% CaO, 0.06% P₂O₅, 0.01% Cr₂O₃, 3.22% Na₂O, and 9.8% loss on ignition. Some impurities like quartz, mica, and feldspar are also present in the sample.

III. 2.2 CHARACTERIZATION TECHNIQUES

To determine the total volatile content (loss on ignition) 50 gm of clay sample was taken and by using muffle furnace at the temperature 700°C for 1 hour the loss on ignition was calculated 9.8% for sodium bentonite. The sodium bentonite sample was characterized by X-Ray Fluorescence (XRF), X-Ray Diffraction (XRD) and Fourier Transformed Infrared Spectroscopy (FT-IR). The elemental analysis data of the clay samples were obtained through XRF PW2400 model of Phillips, scintillation detector having current 40 mA, voltage 40 mV, and rhodium anode X-ray tube. A Rigaku ULTIMA IV Powder X-Ray Diffractometer was used for XRD data collection with 2 θ measuring range -3° to 162°(maximum), minimum step size 0.0001°, goniometer radius of 285 mm, X-ray generator of maximum rated output 3 kW, rated tube voltage 20-60 kV, focus size 0.4 × 12 mm and employing Bragg-Brentano and parallel beam optics. The XRD pattern was obtained at room temperature in the range of 10° to 90°, with basic accuracy $\pm 2^\circ$. X-ray of wavelength 1.540598 Å is applied. FT-IR high-resolution data were collected by using a Model- SPECTRUM 100 of Perkin Elmer, auto-calibrated and traceable to AnC-38. The Model has accessories HATR (horizontal attenuated total reflection) and DRIFT (diffuse reflectance system). Data is recorded on K-Br pellets with a resolution of 4 cm⁻¹ in the range of 450 cm⁻¹ to 4000 cm⁻¹ SEM analysis was recorded by LEO S430 scanning electron microscope attached with energy dispersive X-ray analyzer model OXFORD LINK ISIS. Model STD 2964 computerized TA machine was used for thermal analysis and α -Al₂O₃ was used as the reference material under atmospheric conditions.

IV. 3. RESULTS AND DISCUSSIONS

3.1 Loss on ignition test (LOI)

50 gm of each sample was taken for the loss on ignition test. Most of the researchers used the kaolin clay in alteration of plastic wastes to gain useful hydrocarbons tested for liquid transportation fuel. The pyrolysis technique was used by several for temperature ranges from 500°C to 800°C. The degradation process of plastic wastes besides with catalyst can be done to obtain high-quality products at low temperature [10]. Sodium bentonite has 9.8% LOI by weight. Muffle furnace was set on before doing a test for two hours to reach the temperature at 900°C. Kaolin clay sample and sodium bentonite samples of 50 gm were treated for 1 hour separately and weighed as 44 gm and 45.1 gm respectively by using electronic weight measuring instrument. This is done three times for separate parent clay samples. Less value of LOI for sodium bentonite shows that the acceptance performance as a catalyst using in waste plastic valorization is better than the kaolin clay. The pyrolysis technique was used by several for temperature ranges from 500°C to 800°C. The degradation process of plastic wastes besides with catalyst can be done to obtain high-quality products at low temperature [10]. Sodium bentonite has 9.8% LOI by weight.

3.2. X-ray Fluorescence Characterization

The XRF data of sodium bentonite shows that the base anhydride of sodium hydroxide Na₂O is richer than the kaolin sample, which is the useful sign for using as a catalyst in the waste valorization of plastics, has good tendency to enhance the pyrolysis process. Figure 1 shows the chemical compositions of high contents. Nickel (II) oxide is also traced which clarifies that the sodium bentonite has an important role in the pyrolysis process, however, Li et al. studied that the weight loss of biomass components occurred at low-temperature range and reduction in activation energy was observed. Also, Nano-NiO has a better catalytic effect than micro-NiO particles [11]. Table I represents the components of the sodium bentonite for the studied sample. The influence of CaO as a catalyst was studied by Investigations showed that the CaO plays an important role in pyrolysis for better outcomes [12-15]. The rich presence of CaO enhances the quality behaviour of sodium bentonite over clays. Existence of magnesium oxide is supporting the good catalytic behaviour of sodium bentonite in the pyrolysis reaction. [15-17].

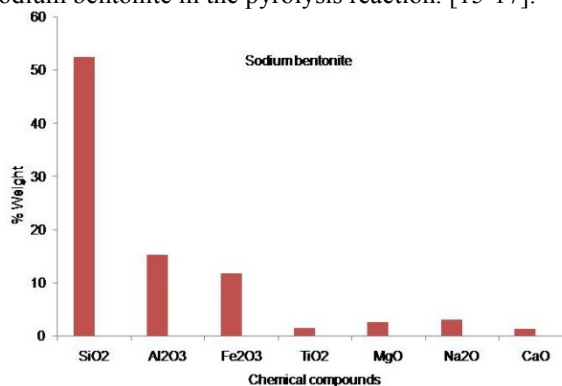


Figure 1. Major chemical compounds present in the clay sample

TABLE I
Compositions of Clay samples based on XRF (in weight (%))

Sodium bentonite	
Chemical compounds	%WEIGHT
SiO ₂	52.55
Al ₂ O ₃	15.34
K ₂ O	0.290
Fe ₂ O ₃	11.92
TiO ₂	1.620
MgO	2.750
Na ₂ O	3.220
CaO	1.400
P ₂ O ₅	0.060
Cr ₂ O ₃	0.010
NiO	0.020

3.3. FT-IR characterization of sodium bentonite

In this study from the IR spectra of the sodium bentonite, the absorption band at 3695.17 cm⁻¹ is due to stretching vibration of O-H groups and relates to alcohols and phenol type of compounds shown in figure 2. A sharp band appears caused by the Si-O-H vibrations of photon energy.

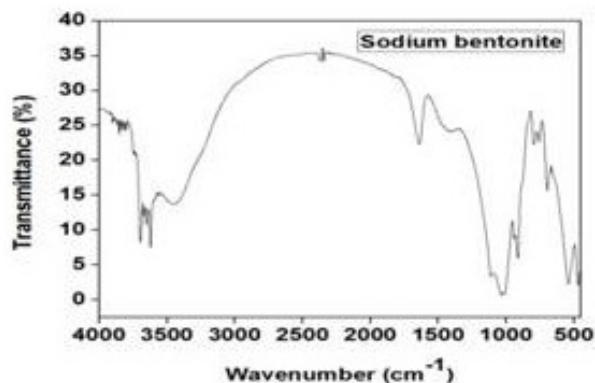


Figure 2. FT-IR spectra of sodium bentonite clay

The band positions at 3445.87 cm⁻¹ and 3620.59 cm⁻¹ are due to H-O-H vibrations of water absorbed on the clay surface as well as vibrations of Si-O-H from the solid. Table 3 shows the IR band positions of the sodium bentonite due to different vibrations. The appearance of a band position at 796.59 cm⁻¹ due to Al-Mg-OH stretching confirms the presence of quartz and has been confirmed by X-ray diffraction also. Two weak bands at 938.81 cm⁻¹ and 1421.46 cm⁻¹ are due to O-H bending of a carboxylic acid group and C-H bending of alkanes. A weak narrow band of 2380.24 cm⁻¹ confirms the CO₂ group of compounds. Broad, strong broad and medium sharp bands of 698.49cm⁻¹, 539.26 cm⁻¹, and 470.79 cm⁻¹ are due to Si-O, Si-O-Al, and Si-O-Si stretching.

3.4. X-Ray Diffraction Characterization of sodium bentonite clay

The absorption peaks found at 2 θ (°) = 5.71°, 7.61°, 12.55°, 19.89°, 20.53°, 21.03°, 21.42°, 25.09°, 35.05°, 35.92°, and 61.69° shown by the IR spectra in figure 3. The maximum peak appears at 12.55°. Full Width at the half-maximum value (FWHM) is the same for the two absorption peaks at 5.71 Å and 7.61 Å. The average crystallite size (D_p) is maximum at 25.09° of absorption. The XRD pattern shows the presence of low quartz and silicon oxides at different absorptions which also

satisfy the XRF analysis. Triclinic (anorthic), monoclinic, cubic and orthorhombic crystal structures at different absorptions reveal the phase identification of the sample.

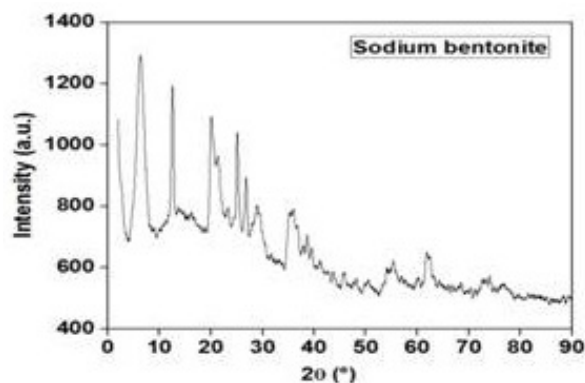


Figure 2. XRD of sodium bentonite clay

3.5. Scanning electron microscopy (SEM) analysis of sodium bentonite

The morphological features have been reported in the scanning electron micrograph. The morphology indicates that the presences of large particles are in the form of agglomerates. More weight % of CaCO₃ and SiO₂ is spotted in spectrum 1 as shown in figure 4. The micrograph shows that flaky particles are stacked together. Broken edges are reported in the SEM image and a large number of clay particles are reported with Fe, Ti, Mg, and Al.

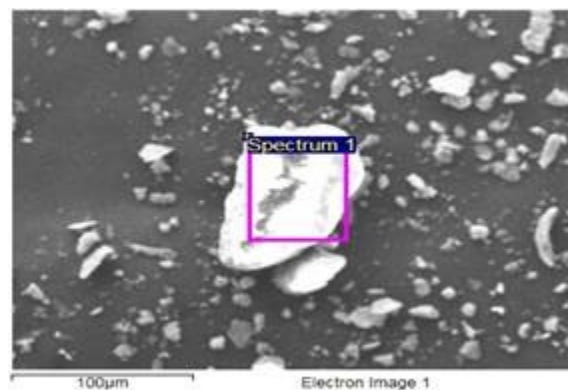


Figure 4. SEM image of sodium bentonite

3.6 TGA and DSC (Differential scanning calorimetry) analysis of sodium bentonite

The thermo gravimetric curves for acid-treated sodium bentonite were depicted in figure 5. The initial sharp fall is due to the continuous loss of hydroxyl groups and hydration water at 110°C. The average degradation of sodium bentonite occurs between 400°C to 550°C. The curve shows that the negligible weight loss is above 650°C. The heat flow gradually increases up to 400°C and a sharp fall is recorded up to 800°C as recorded in figure 6. The glass transition occurs in between 0°C to 100°C and the crystallization range is 200°C to 400°C. The melting occurs about to after 450°C it satisfies the XRD results. The sodium bentonite is had more and more possibilities as a beneficial catalyst for the plastic waste pyrolysis process. As the pyrolysis is endothermic reaction occurs in the absence of oxygen the required heat flow is beneficial in case of sodium bentonite.

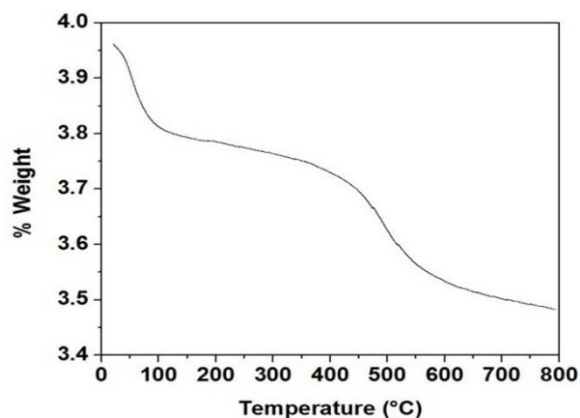


Figure 5. TGA graph of HCl treated sodium bentonite

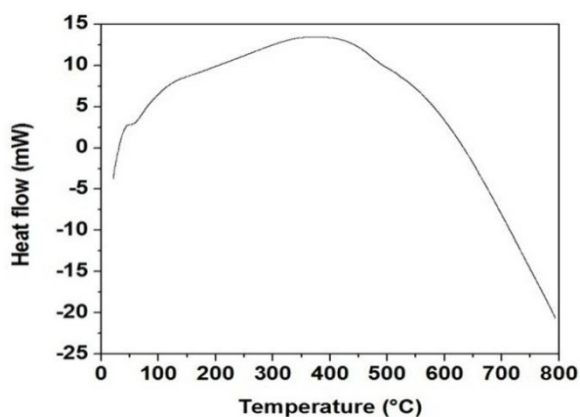


Figure 6. DSC graph of HCl treated sodium bentonite

V. 4. CONCLUSIONS

The analysis of sodium bentonite clay sample using XRF, FT-IR, XRD and SEM instruments have shown the prominent nature of the clay further useful as the alternate catalyst for plastic waste valorization. The commercially available clay is cheap and has better acceptable for the pyrolysis process. As the presence of alumina and silicate compositions are found from the XRF and the results of XRF supported by XRD, FT-IR and SEM analysis. Average crystallite size is found as 26.55 nm at the 25.09° of absorption, by XRD analysis. TGA and DSC curves satisfy the reliability required temperature range for useful waste plastic valorization using sodium bentonite as a catalyst.

References

- [1] Asad, A., Shantanu, K., Mohammad, A.D. and Raquibul, H. (2013); Suitability of Bentonite Clay: An Analytical Approach. *International Journal of Earth Science*, 2(3): 88-95.
- [2] Ahmed A.S, Salahudeen, N., Ajinomoh, C.S., Hamza, H. and Ohikere, A. (2012); Studies on the Mineral and Chemical Characteristics of Pindiga Bentonitic Clay. *Petroleum Technology Development Journal* (ISSN 1595-9104). An International Journal. 1: 1-8.
- [3] Tijen, S. (2010); Purification and Modification of Bentonite and its use in Polypropylene and Linear Low-Density Polyethylene Matrix Nanocomposites. A PhD thesis submitted to the Chemical Engineering Department, Middle East Technical University.
- [4] Ahonen, L., Korkeakoski, P., Tiljander, M., Kivikoski, H. and Rainer L.(2008); Quality Assurance of the Bentonite Material. POSIVA OY Working Report 33.
- [5] RMRDC Raw Materials Research and Development Council (2007), Technical Brief on Mineral Raw Materials in Nigeria –

Bentonite, Revised edn., Abuja.

[6] James O. O., Adediran, M. M., Adekola, F. A., Odeunmi, E. O. and Adekeye, J. I. D. (2008); Beneficiation and Characterisation of a Bentonite from North-Eastern Nigeria. *Journal of the North Carolina Academy of Science*, 124(4):154–158.

[7] Trauger, R.L (1994); The Structure, Properties and Analysis of Bentonite in Geosynthetic Clay Liners. *Geosynthetic Resins, Formulation and Manufacturing. Proceedings of 8th GRI Conference.*

[8] Holtzer, M., Bobrowski, A. and Grabowska, B. (2011); Montmorillonite: A Comparison of Methods for its Determination in Foundry Bentonites, *Metabk* 50(2):119-122.

[9] Vingas, G.J., Zrimsek, A.H., 1964. Thermal stability of bentonites in foundry moulding sand. In: *Proceedings of the 13th National Conference on Clays and Clay Minerals*, pp. 367–380.

[10] Miskolczi N, Bartha L, Deak Gy, Thermal degradation of polyethene and polystyrene from the packaging industry over different catalysts into fuel-like feedstocks, *Polymer degradation and stability*, 2006:517-526.

[11] Jianfen Li, Rong Yan, Bo Xiao, David Tee Lang, and Dong Ho Lee, Preparation of Nano-NiO particles and Evaluation of their Catalytic Activity in Pyrolyzing Biomass Components, *Energy and fuels*, vol.22:, Issue. 1,: pages 16-23, 2007.

[12] Wu, D., Zhang, S., Zheng, Q., Zheng, Q., Zhao, X., Liu, W., Xue, X., The influence of CaO on the Pyrolysis Behaviour and kinetic Characteristics of Low-Rank Coal., *Energy Procedia*, Volume 105,2017.

[13] Guan Rengui, Li Wen, Li Baoqing, Effects of Ca-based additives on pyrolysis of Datong coal [J], *Journal of China University of Mining and Technology*, 31 (4) (2002), pp. 396-401.

[14] Zhu Ting Yu, Lui Li Peng, Wang Yang, et al., Study on coal mild gasification with Cao catalyst [J], *Journal of Fuel Chemistry & Technology*, 2000,28(1): 36-39.

[15] Ersan Putin, Catalytic pyrolysis of biomass: Effect of pyrolysis temperature, sweeping gas flow rate and MgO catalyst, *Article in Energy* 35(7): 2761-2766, July 2010.

[16] S.A. Karakoulia, K.G. Kalogiannis, et al., Natural magnesium oxide (MgO) catalysts: A cost-effective sustainable alternative to acid zeolites for the in situ upgrading of biomass fast pyrolysis oil, *Applied Catalysis B: Environmental*, Volume, 196, 2016, pp. 155-173.

[17] Jungjaroenpanit C., Vitidsant T., Catalytic pyrolysis of used cooking oil by magnesium oxide supported on activated carbon in a continuous reactor, *International journal of chemical Environmental and biological sciences*, volume: 1 pp.429-432, 2013.